Analyst

PAPER

View Article Online
View Journal | View Issue

Cite this: *Analyst*, 2023, **148**, 5731

An ion-selective chemiresistive platform as demonstrated for the detection of nitrogen species in water†

Maryam Darestani-Farahani, [a] Fanqing Ma,[a] Vinay Patel, [b] Ponnambalam Ravi Selvaganapathy [b] and Peter Kruse *[a]

The use of ion-selective electrodes (ISE) is a well-established technique for the detection of ions in aqueous solutions but requires the use of a reference electrode. Here, we introduce a platform of ion-selective chemiresistors for the detection of nitrogen species in water as an alternative method without the need for reference electrodes. Chemiresistors have a sensitive surface that is prone to damage during operation in aqueous solutions. By applying a layer of ion-selective membrane to the surface of the chemiresistive device, the surface becomes protected and highly selective. We demonstrate both anion-selective (NO_3^-, NO_2^-) and cation-selective (NH_4^+) membranes. The nitrate sensors are able to measure nitrate ions in a range of 2.2–220 ppm with a detection limit of 0.3 ppm. The nitrite sensors respond between 67 ppb and 67 ppm of nitrite ions (64 ppb detection limit). The ammonium sensors can measure ammonium concentrations in a wide range from 10 ppb to 100 ppm (0.5 ppb detection limit). The fast responses to nitrate and nitrite are due to a mechanism involving electrostatic gating repulsion between negative charge carriers of the film and anions while ammonium detection arises from two mechanisms based on electrostatic gating repulsion and adsorption of ammonium ions at the surface of the p-doped chemiresistive film. The adsorption phenomenon slows down the recovery time of the ammonium sensor. This sensor design is a new platform to continuously monitor ions in industrial, domestic, and environmental water resources by robust chemiresistive devices.

Received 25th July 2023,
Accepted 9th October 2023

DOI: 10.1039/d3an01267k

rsc.li/analyst

1. Introduction

In order to maintain or improve water quality, it must be monitored. This requires designing a general, robust and cost-effective platform which can measure several parameters in water,[1–3] such as pH, water hardness, dissolved oxygen, oxidation reduction potential (ORP), disinfectants, forms of nitrogen such as nitrate, nitrite and ammonium, phosphorus, sulfur, micronutrients and heavy metals online, *in situ* and real time.[4] Among these parameters, nitrogen species are particularly important and play a critical role to sustain nutrients in aqueous ecosystems. It is therefore essential to ensure their concentrations in water are in balance.[5] High levels of these compounds cause eutrophication in the environment and are detrimental to human health.[6–9] The WHO has set the maximum acceptable concentrations for nitrate and nitrite ions in drinking water to be 50 ppm and 0.2 ppm, respectively.[4,6] The proposed threshold for ammonium ions in drinking water is 35 ppm.[10] For continuous water analysis of these ions, the two common ion sensing platforms which have been commercialized so far are electrochemical devices, in particular potentiometric sensors, and spectroscopic methods, especially colorimetric sensors.[6,8] Although many promising approaches have been proposed in the literature, they still suffer from some significant shortcomings.[11] For instance, electrochemical devices require reference electrodes.[12] Colorimetric sensors often suffer from matrix effects and require additional reagents to react with the analyte.[13] Ion-selective field effect transistor (ISFET) sensors have been demonstrated in the laboratory to have potential to be miniaturized and embedded on a chip for ion detection, although they still require reference electrodes for operation.[14–17] These devices have demonstrated good performance for ion detection in water but their complex structure makes them expensive to fabricate, elaborate to operate, and prone to failure.[13] Hence, there is still a need for an easy to fabricate, robust detection system which does not require a reference electrode or any reagents.

Chemiresistive devices are an alternative approach for ion detection in water.[13] They are a type of solid-state electrical

[a]*Department of Chemistry and Chemical Biology, McMaster University, 1280 Main Street West, Hamilton, Ontario L8S 4M1, Canada*
[b]*Department of Mechanical Engineering, McMaster University, 1280 Main Street West, Hamilton, Ontario L8S 4L7, Canada. E-mail: pkruse@mcmaster.ca*
† Electronic supplementary information (ESI) available. See DOI: https://doi.org/10.1039/d3an01267k

sensors whose resistance is modulated upon interacting with the analyte.[18,19] They can be thought of as a simplified form of FET devices operating at zero gate voltage.[20] It is important to note that the working principle of this electrical method of analysis is different from conductometry or amperometry. In conductometric and amperometric methods, the current is flowing through the solution while in electrical sensors such as FETs and chemiresistive devices the current is flowing through the resistive film parallel to the electrochemical double layer (EDL), never entering the solution. Instead, changes in the EDL modulate the electronic properties of the resistive film, hence its surface properties are of significance. Furthermore, this is why the response of chemiresistive sensors is not diffusion controlled. Conductometric devices measure changes in conductivity of an analyte-containing electrolyte without the use of a reference electrode.[21] Amperometric sensors measure changes in current through an electrode in contact with the analyte solution as a result of an electroactive substance losing or gaining electrons while undergoing a redox reaction. The sensing process of this type of sensors is diffusion controlled and involves a reference electrode.[22] In conductometric and amperometric sensors, the applied voltage and resulting current through the analyte can interfere with the response of the sensor, while chemiresistors can operate non-destructively at much lower voltages and without any current flowing through the analyte. Therefore, the chemiresistive method can be a safer choice with simpler geometry to measure the analyte. Chemiresistive sensors have been commercialized for gas detection,[23] but they are not commonly deployed in aqueous solutions due to their sensitivity to pH and ionic strength, the need to avoid electrochemical side reactions and electrolytic water splitting in addition to non-specific bindings and low interaction energy between analyte and the resistive film in water.[4,24] Some chemiresistive sensors have been developed in our research group for the measurement of different analytes such as free chlorine,[25–27] silver,[13] phosphate[28] and pH.[29] In free chlorine measurement, other oxidants might interfere with free chlorine detection.[25] Copper interferes with the silver sensor.[13] Some fabricated sensors were tested for nitrate, nitrite and ammonium but they were either not sensitive or not selective to these analytes. Hence, no chemiresistors for the detection of nitrogen species have been fabricated yet.

These challenges of chemiresistive devices in aqueous solutions can be overcome by covering the surface of the chemiresistive films with an ion-selective membrane (ISM) to protect sensors surfaces in water and interact selectively and reversibly with target analytes.[30,31] These can be the same type of ISMs that are commonly used in ion selective electrodes (ISEs)[32] or conductometric devices.[33,34] Cammann *et al.* have demonstrated an elegant application of conductometry by using an ISM to selectively pre-concentrate analyte ions and then measuring the change in conductivity of the ISM.[33,34] In the conductometric devices developed by the Cammann group, the ISM is part of the electric circuit for detection, which requires the application of higher voltages and will cause reactions (and side reactions) involving the analyte and membrane components. In contrast, chemiresistive devices detect changes in the electric conductivity of the resistive film as a result of its interactions with an analyte (or ISM) that itself is not part of the electric measurement circuit. The analyte and the components of the membrane are not impacted by the detection process.

In this study, a family of ion-selective chemiresistive sensors for the detection of nitrogen species were demonstrated for the first time. They consist of conductive CNT networks coated with appropriate ISMs to detect anionic and cationic target analytes in water. The thicknesses of the CNT film and the ISM were optimized. Sensitivity, selectivity, and reproducibility tests were done to validate sensor performance, establish the sensing mechanism for each analyte and compare sensor operation to the potentiometric method as a reference method. This design eliminates the need for a reference electrode compared to potentiometric ISE devices and improves the selectivity and stability of the device.

2. Experimental

2.1. Materials, reagents and samples

Single-walled carbon nanotube powder ((6,5) chirality, carbon content ≥95%, ≥93% carbon as SWCNT, 0.7–0.9 nm diameter) was purchased from Sigma Aldrich and used without additional purification. Sodium nitrate was purchased from Caledon. Sodium nitrite, ammonium chloride, ammonium sulphate, sodium hydroxide, potassium chloride, hydrochloric acid, glacial acetic acid, tris(hydroxymethyl)aminomethane base, 3-(trimethoxysilyl)propyl methacrylate (TPM), poly(vinyl-chloride) (PVC, high molecular wt), nitrite ionophore(IV) (cobalt(II) *tert*-butyl-salophen), tridodecylmethylammonium nitrate (TDMAN), tridodecylmethylammonium chloride (TDMACl), nonactin, potassium tetrakis(4-chlorophenyl) borate, bis(2-ethylhexyl)sebacate (DOS), 2-nitrophenyl octyl ether (*o*-NPOE), and tetrahydrofuran (THF) were purchased from Sigma Aldrich. Ultrapure water (18.2 MΩ cm) was supplied by a Millipore Simplicity UV water purifier. All organic solvents such as methanol were HPLC grade. An environmental sample was collected from Spencer Creek in Hamilton, Ontario, Canada.[35]

For CNT preparation, a mixture of 5 mg SWCNT and 15 ml methanol was sonicated in a bath sonicator (Elmasonic P30H ultrasonic cleaner) for 6 h at 37 kHz (100% power) and 30 °C on the sweep setting.[36] After CNT dispersion, 2 ml of the suspension was isolated and 6.67 mg of TPM (CNT : TPM in a ratio of 1 : 20) was added to it. The mixture was sonicated at 37 kHz (100% power) and 30 °C on the sweep setting for 4 hours. To observe their morphology, a film of pristine CNT and a CNT–TPM film were fabricated by air-brushing the respective dispersed solutions onto 1 × 1 cm^2 pieces of SiO_2-covered Si wafer until resistances between 4 kΩ and 5 kΩ were obtained. Then, the prepared samples were sputter coated with 5 nm platinum and characterized by scanning electron microscopy

(SEM) in a JEOL JSM-7000F at 3 kV. SEM images and properties of the conductive layer (resistive film) are discussed in the Results section.

Acetic acid was prepared by diluting 99.7% glacial acetic acid (ACS reagent grade) into ultrapure water. The concentrations of the standard solutions were confirmed using an Orion Aquamate 8000 UV-Vis spectrophotometer and Thermo Scientific Orion AQUAfast II test kits for nitrate, nitrite and ammonium. For membrane solution preparation, the required mass of each component was weighed and dissolved in 2 mL of THF.

For device fabrication, frosted glass slides (75 × 25 × 1 mm^3, ground edges, pre-cleaned twin frosted end, VWR), a 9B pencil, $\frac{1}{4}''$ wide EMI copper foil shielding tape (3M #1181), polydimethylsiloxane (PDMS) (Sylgard 184 silicon elastomer kit including base : curing agent mixed in a 10 : 1 ratio) were also used.

2.2. Sensor fabrication

Mixtures of ionophore, plasticizer, PVC and additives were used to prepare the cocktail for each ion-selective membrane. For the nitrate-selective membrane cocktail, 6.0 mg TDMAN, 31.3 mg PVC and 62.6 mg *o*-NPOE were dissolved in 2 mL THF.[37] For the nitrite-selective membrane cocktail, 1.1 mg nitrite ionophore(VI) (cobalt(II) *tert*-butyl-salophen), 0.3 mg TDMACl, 32.5 mg PVC and 65.4 mg DOS were dissolved in 2 mL THF.[37] For the ammonium-selective membrane cocktail, 1 mg nonactin, 0.7 mg potassium tetrakis(4-chlorophenyl) borate for a 2 : 1 molar ratio, 33 mg PVC, and 66 mg *o*-NPOE were dissolved in 2 mL THF.[7] The compositions were homogenized on a vortex mixer for 20 minutes.

The sensor fabrication process is shown in Fig. 1. At first, glass slides were cleaned with methanol and hydroxylated in 0.1 M KOH for 30 minutes to prepare the surface for silanation. Then, two rectangular contact pads with dimension 6.5 × 18 mm^2 were drawn on opposite sides of the frosted part with a 9B pencil (Fig. 1a). Afterwards, the CNT–TPM composite was air brushed onto the center of the frosted part using a gravity feed airbrush (neo for Iwata N4500, CN nozzle 0.35 mm) at 10 psi pressure until a resistance between 5 kΩ and 10 kΩ was achieved. Air brushing was performed on a hotplate at 50 °C to accelerate solvent evaporation. The glass slides were then placed into an oven at 110 °C for 90 minutes.[38] After cooling down the devices, resistance was less than 20 kΩ (Fig. 1b). Next, two strips of adhesive copper tape were attached to the pencil contact pads across the glass slide (Fig. 1c) and covered with PDMS (which was prepared 4 to 6 hours prior to application to be viscous enough and avoid spreading over the CNT film) and left on a hotplate at 60 °C for an hour to let the PDMS cure completely (Fig. 1d). Then, 100 μL of ion-selective membrane solution was drop-cast at the center of the conductive layer and left to dry for 12 hours at room temperature (Fig. 1e). The actual images of fabricated sensors in addition to their dimensions can be seen in Fig. S1a.† The effective surface area of the sensors was calculated to be 175 mm^2. The average typical thickness of the membranes was 39 μm, as determined with an Alicona microscope (Fig. S2†).

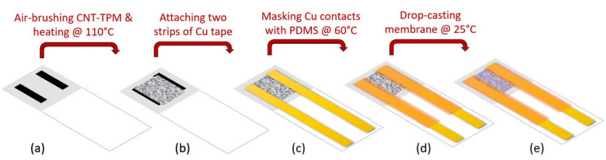

Fig. 1 Sensor fabrication process. (a) Hydroxylated glass slide with pencil contact pads, (b) air-brushed CNT–TPM which was heated at 110 °C for 90 minutes, (c) applied copper contacts in parallel, (d) covered contacts with PDMS and cured at 60 °C for an hour, (e) completed device with ion-selective membrane.

The last step of the process was conditioning the nitrate, nitrite, and ammonium sensors in aqueous solutions containing 200 ppm nitrate, nitrite, and ammonium ions, respectively, for 24 hours in order for ion replacement to occur. After conditioning, the sensors were washed with ultrapure water to ensure all analyte ions were removed and the sensors were ready to use. The final resistances of the films were measured to make sure they are between 20 and 50 kΩ. The resistances of the devices after each fabrication step can be found in Table S1†.

2.3. Data acquisition

For the sensing tests of each analyte, batches of four sensors were fabricated, one sensor of which was blank (covered with a blank membrane which included all membrane components except the ionophore) as a control. They were dipped into 500 mL of background solution in a Pyrex bowl equipped with a stir bar. The bowl was placed on a stirrer (300 rpm) with the sensors arranged along the perimeter of the bowl facing towards the centre. Sensors were connected to a four-channel eDAQ (eDAQ EPU452 quad multi-function isoPod) in "biosensor" configuration to record the current over time (Fig. S1b†). The eDAQ was connected to a computer *via* a USB serial controller for data acquisition and processing. The polarization for each sensor was set at 20 mV to observe a 300–600 nA current in a set 2000 nA range.

During the initial set-up of each experiment, sensors were left overnight to equilibrate in the background solution (14–16 h). After reaching equilibrium and a stable baseline, various volumes of stock solution of nitrate, nitrite or ammonium ions were spiked to the bowl such that the range of concentrations of analyte was from 10 ppb to 330 ppm of each ion. Several batches of the sensors were fabricated and tested to ensure reproducibility.

Eqn (1) was used to calculate the response of a sensor, where I_0 is the current of the baseline (average value of last 60 points right before addition) and I is the recorded stable current after 15 minutes of analyte addition in each step (average value of 60 points):

$$\%\text{Response} = \frac{I - I_0}{I_0} \times 100\% \quad (1)$$

For pH and conductivity measurements, a pH electrode and a conductivity electrode were also purchased from eDAQ Inc as

part of an ER7006 multisensor kit. The pH electrode was calibrated using two buffer solutions with pH 4 and pH 7 at 22 °C. The conductivity electrode was calibrated using a 0.1 M KCl solution with a cell constant of 0.1 cm^{-1} at 22 °C.

3. Results and discussion

3.1. Conducting layer (CNT–TPM film)

As explained in the fabrication section, the chemiresistive devices have a conductive layer (or resistive film) which is connected to two copper contacts at either end and exposed to the target analyte such that only the conductive layer and not the contacts interact with the ions.[13] The surface of the chemiresistive devices plays the most important role in their sensing response. Thus, it needs to be deposited as uniformly and as reproducibly as possible. Single-walled carbon nanotubes (SWCNTs) were selected as the conductive layer (Fig. 2a and b) due to their solution processability and high specific surface area.[39] CNTs are very sensitive ion-to-electron transducers in solid-state devices which enhances the output stability and response rate.[40–43] Hence, cost-effective, miniaturized and flexible sensors can be made with CNTs.[44] At ambient conditions, CNTs are p-doped due to adsorption of oxygen molecules in air,[45–47] making p-type CNT films easier to prepare than n-type CNT films.[48]

Mechanical stability can be an issue during fabrication due to hydrophobicity differences between the glass slide, the CNT layer and the membrane, requiring the use of an adhesive material such as alkoxy-silane compounds to improve adhesion between these surfaces.[49] Here, CNTs were mixed with 3-(trimethoxysilyl)propyl methacrylate (TPM) as a coupling agent, sonicated for four hours and cured at 110 °C for 90 min (Fig. 2c and d).[38] This procedure not only solved the adhesion problem in the fabricated devices but also resulted in a uniform and well-distributed film compared to pristine CNTs (Fig. 2d) because TPM functionalized CNTs form a more stable suspension.[50–54] This non-covalent functionalization process does not interfere with the CNT electronic structure and preserves the conductivity of the percolation network.[55] Furthermore, Zou *et al.* reported that by sonicating CNT with TPM, TPM was hydrolyzed and condensed to form polysilsesquioxane which acts as a cross-linker between CNTs.[53] Hence, the prepared film is a highly stable assembled CNT network and CNT films treated with TPM were more consistently woven together compared to isolated bundles in the pristine CNT network (Fig. 2a and c). Moreover, CNTs within the CNT–TPM film are more uniformly distributed than pristine CNTs (Fig. 2b and d). For the purpose of sensor fabrication, the CNT–TPM films were then covered with ion-selective membranes containing the respective ionophores for each analyte. To demonstrate the impact of surface modification with TPM on our fabricated chemiresistive sensors, an example of a water layer test on nitrate sensors is shown in Fig. S3.† The device with the unmodified surface does not return to the baseline after inserting the sensor into the background solution, and its performance worsens during the second cycle while the modified device starts from the same baseline every time after immersing in the background solution. In the following sections, the performances of the developed sensors are described.

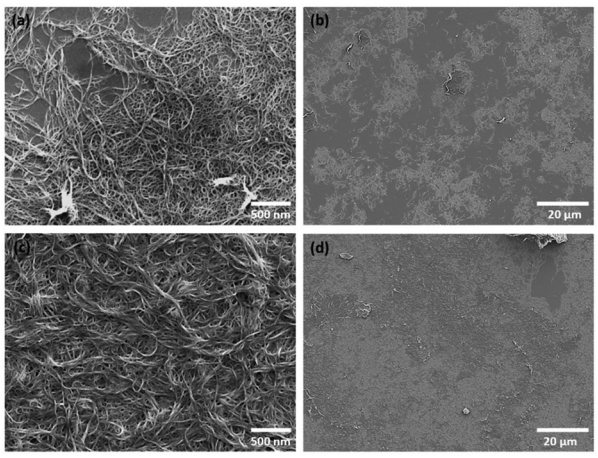

Fig. 2 Zoomed-in and zoomed-out SEM images of (a) air-brushed CNT, scale bar: 500 nm and (b) scale bar: 20 μm, (c) air-brushed CNT–TPM, scale bar: 500 nm and (d) scale bar: 20 μm.

3.2. Performance of nitrate-selective chemiresistive sensors

Every ion-selective membrane solution contains an ionophore that selectively interacts with the target analyte. Moreover, each membrane composition requires a charged component as an ionic site, called a lipophilic additive, to attract the analyte ions electrostatically into the membrane, and to neutralize the charge of the membrane. In the case of nitrate sensing, a commonly used ionophore is tridodecylmethylammonium nitrate (TDMAN) (Fig. S4a†). This quaternary ammonium cation acts as both an ionophore and an ionic site for capturing the nitrate ions, so the additive is not required in this particular membrane composition.[56]

For the sensing experiment, batches of four sensors were fabricated, three of which were coated with a nitrate-selective membrane (100 μL of the cocktail on a 175 mm^2 area) and one of them was covered with a blank membrane (without ionophore, also 100 μL of the cocktail on a 175 mm^2 area). After drop-casting a layer of membrane onto the device, it was conditioned in 200 ppm nitrate solution for 24 h (resistances in Table S1†). The sensors were then immersed in 200 ppm ammonium sulphate (standard method of the U.S. Environmental Protection Agency (EPA)) as background solution overnight.[57] When sensors were equilibrated and the rate of current change decreased below 0.1 pA s^{-1}, the measurement was started, increasing concentrations were added to the bowl and the responses of the sensors were recorded over time. All three nitrate-selective sensors showed a clear step-down behaviour in the current of the resistive film upon exposure to increasing concentrations of nitrate over three cycles while the blank sensor (membrane without ionophore)

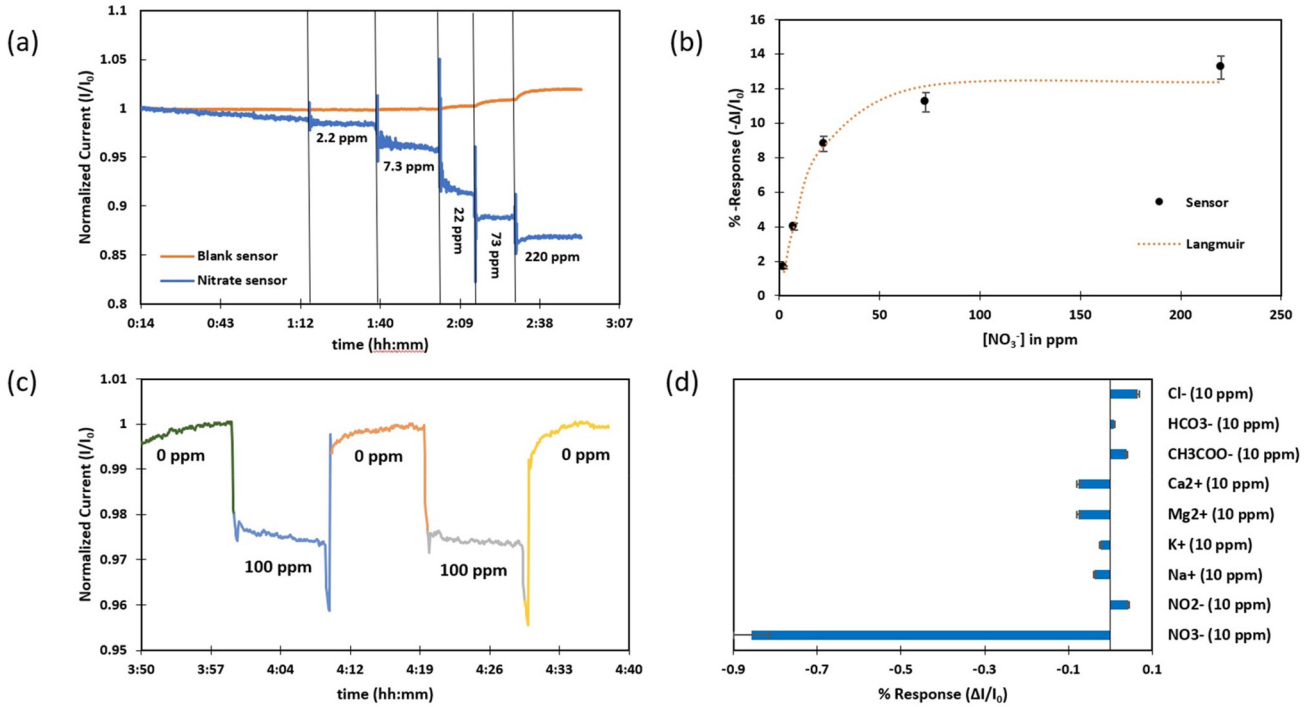

Fig. 3 Performance of the developed nitrate-selective chemiresistive sensor: (a) nitrate response over time in 200 ppm $(NH_4)_2SO_4$ upon addition of elevated concentrations of nitrate ions, (b) calibration curve, (c) reversibility test, (d) interference test.

did not respond (Fig. 3a). The nitrate sensors responded between 2.2 ppm and 220.0 ppm of nitrate ions. This covers the relevant concentration range for real water measurements. Nitrate concentrations range normally between 0–18 ppm in surface water and 4–9 ppm in ground water based on a WHO report but can reach higher levels around 100 ppm depending on soil type, geological situation or agricultural runoff or contaminations by human and animal waste.[10,58,59] A calibration curve for one of the nitrate sensors was plotted according to the amount of response at each concentration *vs.* the ion concentration and data points were fitted to the mathematical model of a Langmuir adsorption isotherm (Fig. 3b).[26] In the Langmuir equation (eqn (2)), c is the analyte concentration in ppm, A represents the maximum response of the sensor and B is a parameter related to the binding equilibrium of the analyte to the sensor (ppm^{-1}) (Table S2†).

$$\%\text{Response} = \frac{ABc}{1 + Bc} \times 100\% \quad (2)$$

From the Langmuir equation, the detection limit of the nitrate sensors was calculated to be 0.3 ppm (3 times the standard deviation of the last 60 points of the baseline before starting the measurement).[60,61] The average response time ($t_{95\%}$) of the sensor was estimated to be 60 seconds by measuring the time required to achieve 95% of the value of the steady current in each step of the measurement.[62] In lower nitrate concentrations, it took longer to get a stable response, but the more analyte is added in the solution, the faster the observed response. Moreover, the RSD of responses of three sensors was obtained as 1.2%.

As the interactions between ion-selective membranes and their specific analytes are generally reversible,[37] our nitrate-selective chemiresistive sensors responded equally well to increases and decreases in concentration (Fig. 3c). This type of reagent-less recovery is highly desirable for continuous measurement applications. To verify their reversibility, the sensors were alternatingly exposed to 0 ppm and 100 ppm nitrate solutions with a 200 ppm ammonium sulphate background for 10 minutes each over three cycles. A fast response (average 52 s) and a fast recovery (average 47 s) were observed at an average recovery rate of 103%.

Selectivity of the fabricated nitrate-selective chemiresistive sensor was high even against chloride which is known as a major interferant for the TDMAN ionophore (Fig. 3d).[3] In order to determine the selectivity of the chemiresistive nitrate sensors, a batch of three nitrate sensors was fabricated and conditioned in a 200 ppm ammonium sulphate solution. Afterwards, 10 ppm each of ions commonly present in water (chloride, bicarbonate, acetate, calcium, magnesium, potassium, sodium, and nitrite) were added sequentially to the solution, followed by 10 ppm of nitrate. No significant response was observed to any of the ions except nitrate.

The influence of the ionic strength on the operation of nitrate sensor, was investigated by measuring the sensor response to 10 ppm nitrate in background solutions with 0, 50, 500 and 5000 ppm of ammonium sulphate (Fig. S5a†). The

sensor response at 5000 ppm background electrolyte decreased to 63.79% compared to the sensor response in 200 ppm background solution. This behavior can be explained by the impact of other ions on the function of the polarity-sensitive ionophore in the membrane before adding nitrate ions as the target analyte. Tridodecylmethylammonium ($TDMA^+$) has a strong affinity for nitrate as a result of the electrostatic interaction and the molecular imprinting effect. The capturing ability of the ionophore for nitrate ions decreases due to existence of more ions at the solution-membrane interface and forming a wider diffuse electric double layer.[63] The performance of the proposed nitrate sensor was studied in a pH range from 4 to 10 (Fig. S5b†). Sensors successfully operated at pH 4 to 8 but a decrease in response was seen at pH 9 and 10 which it might arise from interference by hydroxide ions in high concentration.[64] Hence, for nitrate measurement in real samples, the sensors need to be calibrated with standard solutions at the appropriate conductivity and pH.

3.3. Performance of nitrite-selective chemiresistive sensors

Nitrite-selective chemiresistors were fabricated using a PVC membrane with cobalt(II) *tert*-butyl-salophen as one of the most common nitrite ionophores.[37,65,66] The selected molecule has hydrophilic and electroactive groups to capture the nitrite ion while its exterior part is hydrophobic and interacts with the polymer matrix (Fig. S4b†). Experiments were performed in ammonium sulphate following the EPA guideline for potentiometric determination of nitrite.[67] Four sensors (including three nitrite sensors and a blank sensor, resistances listed in Table S1†) were immersed in 200 ppm ammonium sulphate at pH 5.8. After the sensors reached a steady state current overnight (stability: 0.8 pA s^{-1}), various nitrite ion concentrations were spiked into the background solution, resulting in a drop in conductivity at each step (Fig. 4a) with a measurement range between 67 ppb to 67 ppm and a detection limit of 64 ppb with 2.1% RSD for three sensors. The dynamic range of this nitrite sensor matches with WHO-reported concentrations of nitrite of less than 0.3 ppm in ground water but higher levels in case of contamination which this sensor can detect as high as 67 ppm of nitrite.[10,58] The average response time ($t_{95\%}$) of the nitrite sensors was 103 seconds. The obtained nitrite calibration curve was best fitted to a Langmuir isotherm (Fig. 4b and Table S2†).

The chemiresistive devices coated with nitrite-selective membranes are operating with good reversibility, as expected.[66] Three fabricated devices responded to 67 ppm nitrite in 66 seconds and recovered within 78 seconds with a recovery rate of 102% on average over several cycles (Fig. 4c).

Nitrite-selective sensors exhibited a high level of selectivity, as evidenced by the response of three sensors to 10 ppm of chloride, hydrogen carbonate, acetate, calcium, magnesium, potassium, sodium, nitrate, and finally nitrite (Fig. 4d). Furthermore, the effect of background electrolyte concentration on the response of the nitrite sensor was investigated. Since the ionophore for this sensor is a neutral molecule, the sensor performance is comparable in all tested electrolyte concentrations (Fig. S6a†). Due to the interference of hydroxide with this ionophore[5,68] nitrite measurements must be done in acidic conditions (from pH 3 to pH 6) otherwise no response for nitrite is observed (Fig. S6b†).

3.4. Performance of ammonium-selective chemiresistive sensors

To fabricate ammonium-selective chemiresistive sensors, nonactin was used as a well-known ionophore in a PVC membrane composition.[9,69–71] Nonactin is a cyclic ionophore which has four tetrahydrofuran and four ester groups in its structure. It has 16 stereogenic centers which enables it to form a complex with ammonium in a way that polar and hydrophilic groups point inwards; nonpolar and hydrophobic moieties point outwards (Fig. S4c†).[31] A batch of four sensors including three ammonium sensors and one blank were fabricated (resistances in Table S1†) and tested in 200 ppm Tris-acetate buffer at pH 6 since the ammonium ion dominates over ammonia in equilibria at pH lower than 9.26 ($pK_{a(NH_3/NH_4^+)}$ = 9.26).[70] The prepared devices were left to stabilize overnight and reached a very low current drift rate of 1.7 pA s^{-1}. After beginning the measurement, upon interaction of ammonium ions with the CNT network, the current through the chemiresistor was found to decrease, and the sensor responded from 10 ppb to 100 ppm of ammonium solution (Fig. 5a) with an LOD of 0.5 ppb and RSD of 0.6%. This sensor range covers expected concentrations in real samples since it is reported by the WHO that the natural levels of ammonia/ammonium in groundwater are 0.2–3 ppm and may reach as high as 12 ppm in surface water which is below the upper limit of our reported range.[10,72] The average response time ($t_{95\%}$) was 61 seconds. The ammonium sensors showed a noticeably faster response in lower concentrations, possibly indicative of different sensing mechanisms for ammonium detection compared to nitrate and nitrite. Data was best fitted with the mathematical model of a Freundlich isotherm (Fig. 5b), empirically fitting a non-saturating response.[73] In this model (eqn (3)), m and n are curve fitting parameters without direct physical meaning (Table S2†).

$$\%\text{Response} = mC^{1/n} \times 100\% \quad (3)$$

The ammonium sensor response is shown to be reversible, albeit with lower recovery speed compared to the nitrate and nitrite sensors, possibly due to the different sensing mechanism for ammonium sensors (Fig. 5c). According to the result of the reversibility test, the average response time and recovery time to 10 ppm of ammonium were measured to be around 60 seconds and 900 seconds respectively with a recovery rate of 105%. Although the recovery time of this sensor is longer, it does not require any reagents, pH change or inverse potential to recover the sensor.

Interference testing of the ammonium-selective chemiresistive sensor involved the addition of 10 ppm of common cations presented in the water (sodium, potassium, calcium, magnesium, cobalt, nickel, zinc, cadmium), as well as 10 ppm

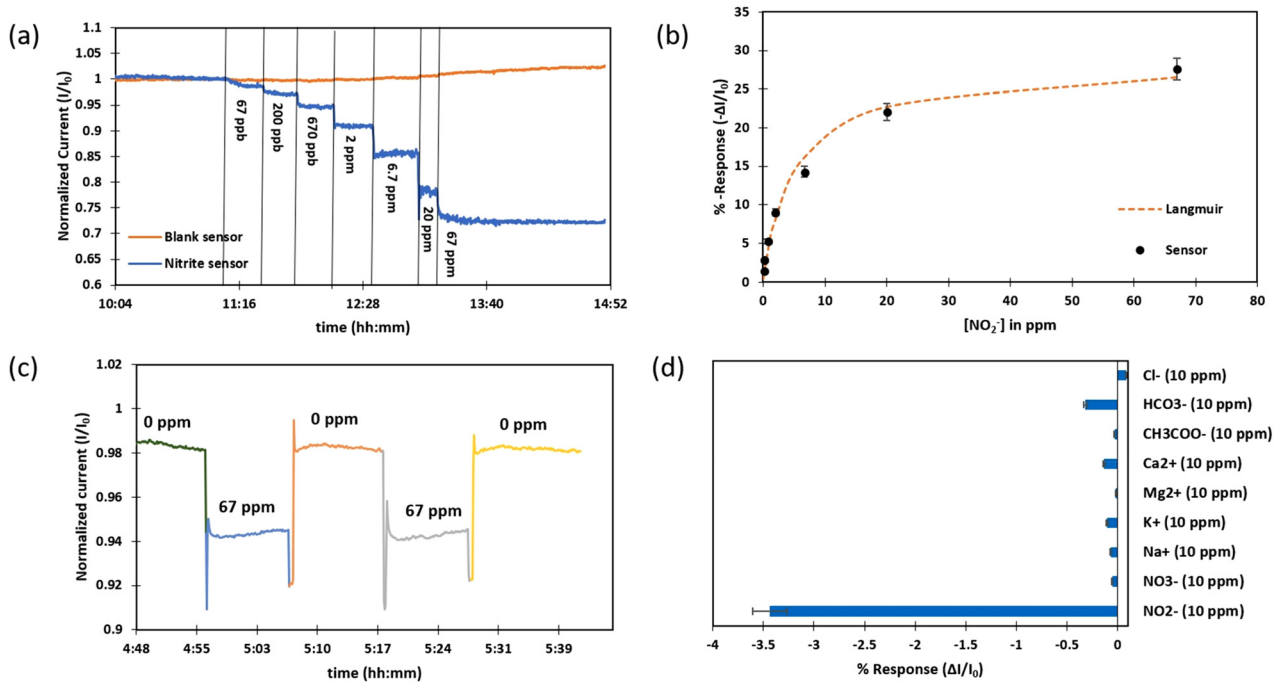

Fig. 4 Performance of the developed nitrite-selective chemiresistive sensor: (a) nitrite response over time in 200 ppm $(NH_4)_2SO_4$ upon addition of elevated concentrations of nitrite ions, (b) calibration curve, (c) reversibility test, (d) interference test.

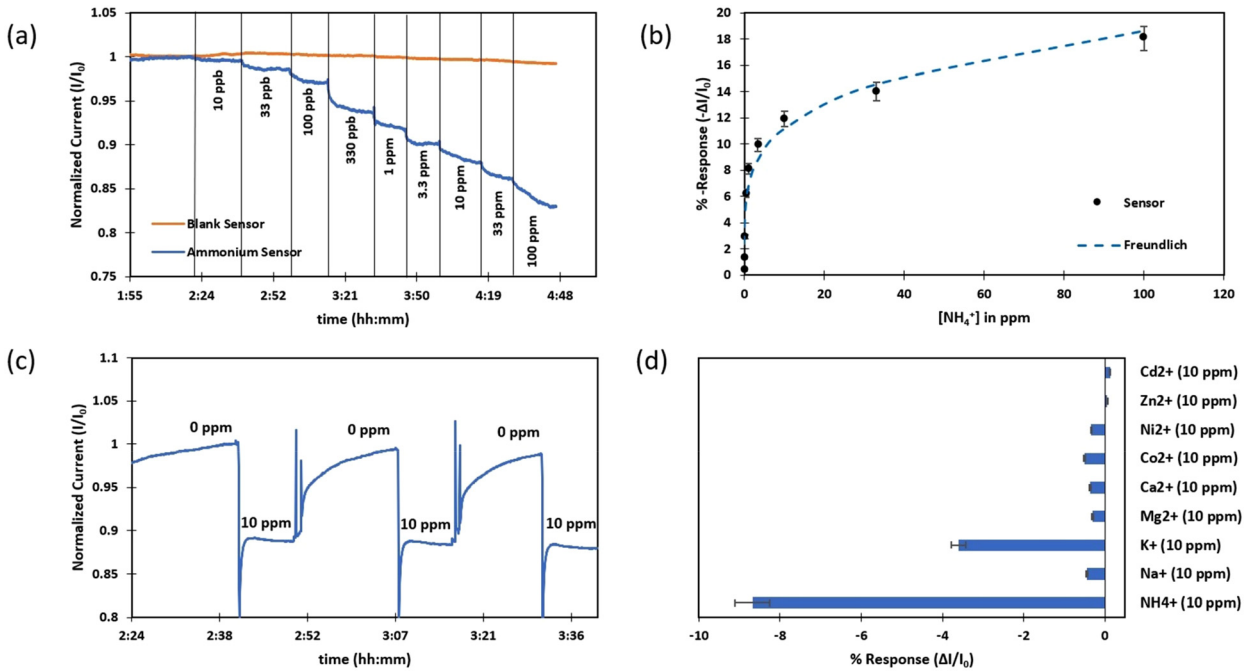

Fig. 5 Performance of developed ammonium-selective chemiresistive sensor: (a) ammonium response over time in 200 ppm Tris-acetate buffer, pH = 7 upon addition of elevated concentrations of ammonium ions, (b) calibration curve, (c) reversibility test by the developed ammonium sensor, (d) interference test.

of ammonium. Averaged responses of three ammonium sensors shown in Fig. 5d which demonstrate the developed ammonium sensor is highly selective to ammonium, with one exception. Ammonium sensors responded about 3.6% to 10 ppm of potassium while the response of the sensor to 10 ppm of ammonium in the presence of potassium and other ions was around 8.3%. K^+ ions are commonly reported in the literature as a substantial interferant for the ammonium-selec-

tive membrane during potentiometric measurements since K^+ ions are very similar in size to ammonium ions and can be captured by nonactin.[69,74] The interfering effect of K^+ was investigated in more detail. When ammonium and potassium were present simultaneously in the solution, the ionophore was found to preferably interact with ammonium and not respond to potassium (Fig. S7a†). Potassium was sensed only in the absence of ammonium (Fig. S7b†). As seen in Fig. S7a,† no response was observed upon the addition of 9 ppm of potassium to a solution already containing 1 ppm of ammonium and 1 ppm of potassium. Another set of experiments was done to examine the interference of potassium in both techniques in separate solutions. In chemiresistive measurements, the concentration of potassium should be on average 92 times higher than the concentration of ammonium to result in the same response of the ammonium sensor (Fig. S7c†). In a set of potentiometric measurements using that same ammonium sensor acted as an ammonium-selective electrode *vs.* a reference electrode, requiring a potassium concentration about 11 times higher than the ammonium concentration to result in the same magnitude of response (Fig. S7d†). Potassium is therefore an interferent for our ammonium-selective chemiresistive sensors, but much less so than for potentiometric sensors, due the difference in sensing mechanism.

The ionic strength of the background electrolyte was not found to affect sensor performance (Fig. S8a†) because nonactin is a neutral molecule like the nitrite ionophore. The performance of three ammonium sensors was tested in different pHs ranged from 4 to 10 (Fig. S8b†). Sensors responded to 10 ppm ammonium at pH 4–9 and worked with the same sensitivity although at pH 10, a drop in the sensor response was seen since it is above its pK_a (9.26) and a portion of the ammonium ions has been converted to ammonia, which is not captured by nonactin.

3.5. Alternative nanocarbon film substrates

Graphene-like carbon (GLC) sheets were used as alternative chemiresistive films to confirm that other p-doped nanocarbon materials show the same behaviour as pristine SWCNTs in our proposed sensing platform. They are few-layer graphene platelets which have been embedded onto the surface of polyethylene terephthalate sheets mechanically without using a binder, so the level of defects is very low in this material.[75–77] Nominally 12 nm thick GLC films (3M Canada) were incorporated into several devices since this thickness provides the desired resistance range.[26] In Fig. S7,† it can be observed that all nitrate, nitrite and ammonium sensors responded qualitatively the same way as pristine CNT, albeit with less sensitivity. The advantage of using 12 nm thick GLC was the consistency in the results between different sensors since the thickness and morphology of the substrate were very well controlled and equal in all fabricated devices.

A range of materials, such as semiconductors and nanocarbon films can be used as substrates. This sensing platform is highly cost-effective because it doesn't require a reference electrode inside the ion-meter. The fabrication cost breakdown per sensor in this study is estimated in Table S3† to be about a dollar per sensor in lab-scale expenses while mass-produced sensors will cost much less than a dollar. This compares favourably to currently available ion selective electrode prices of several hundred dollars. Furthermore, the developed device is consuming ultra-low electric power of less than 10 nW (as a typical sensor power consumption is 20 mV × 400 nA = 8 nW during measurement only) which is an important requirement for a sensor.

3.6. Real sample tests

The fabricated solid-state sensors were also tested in river water collected from Spencer Creek in Hamilton and filtered through 0.2 μm Waltman filter paper to remove solid particles from the samples before measurement. Conductivity and pH of the river water sample were measured to be 0.78 mS cm^{-1} and 8.3 respectively. A nitrate sensor, a nitrite sensor and an ammonium sensor were fabricated and run in the river water sample for several hours to reach a steady state. After that, calibration curves for these sensors were constructed from measurements in prepared standard solutions containing 3, 10, 30 and 100 ppm of analyte (separately for nitrate, nitrite, and ammonium). At the end, a certain concentration of each analyte was spiked in the real samples for three measurements (n = 3). The sensor responses to the river water were converted into concentrations using the calibration curves and compared to the values found with colorimetric standard method (Table 1).

The pH did not need to be adjusted for the nitrate measurement since pH 8.3 is within the operating range of our sensors

Table 1 Real sample analysis for the nitrate, nitrite and ammonium sensors

	Added analyte (ppm)	Found by sensor (ppm)	Found by spectrophotometry (ppm)	Recovery (%)
Nitrate	0	<2.4	<1	—
	30	26.4 ± 6.7	30.3	87.0 ± 22.2
	100	93.7 ± 2.5	98.8	94.9 ± 2.6
Nitrite	0	<0.07	<0.01	—
	30	32.8 ± 1.4	31.2	105.0 ± 4.3
	100	97.4 ± 1.1	99.1	98.3 ± 1.2
Ammonium	0	<0.01	<0.02	—
	10	10.5 ± 0.2	9.87	106.3 ± 1.6
	100	97.0 ± 2.6	99.6	97.4 ± 2.6

(Fig. S5b†). After constructing the calibration curve for nitrate, river water samples were spiked with 30 ppm and 100 ppm of nitrate and three chemiresistive measurements were taken. Recovery for 30 ppm and 100 ppm nitrate solutions was 87.0 ± 5.2% and 94.9 ± 2.6% respectively. The low recovery rate is due to the decreased sensitivity of the nitrate sensors in samples with higher ionic strength (Fig. S5a†).

The nitrite sensors perform best in an acidic environment. Thus, the pH of the samples was adjusted to 6 (Fig. S6b†). After obtaining a calibration curve as described, 30 ppm and 100 ppm of nitrite were spiked into river water samples and measured chemiresistively. The recoveries of 105.0 ± 4.3% and 98.3 ± 1.2% respectively are acceptable values with a very low error range.

The ammonium test was done directly in the river water sample without any added reagents at pH 8.3 since this sensor works in a wide range of pH (Fig. S8b†). The responses to the sample itself, and the sample spiked with 10 and 100 ppm ammonium were recorded and compared to the ammonium calibration curve. The concentrations were also verified colorimetrically. The percentage of recovery for 10 ppm of ammonium was 106.3 ± 1.6% and for 100 ppm was obtained 97.4 ± 2.6%, showing the chemiresistive measurements to be in good agreement with the standard method.

3.7. Comparison to ion-selective potentiometric performance

To directly compare the sensing performance and mechanisms in chemiresistive and potentiometric modes, the same devices can be operated as solid-contact ion-selective electrodes (SC-ISE). Monitoring potentiometric changes during the analyte measurement can give us information about the membrane potential. For this purpose, both copper contacts of our devices were connected to each other to operate the device as a single ion-selective electrode (Fig. 6a and b). A double junction Ag/AgCl electrode was used as a reference electrode. Both electrodes were connected to one eDAQ channel in voltmeter mode. As the concentration of the analyte ions changes, the membrane potential follows a Nernstian behavior. At elevated nitrate and nitrite concentrations, the membrane potential was getting more negative and the potential difference between working electrode (ISE) and reference electrode was decreasing (Fig. 6c and S8a, b†). In contrast, potentiometry tests of ammonium-selective devices showed an upward trend upon exposure to positively charged ammonium ions (Fig. 6c and S8c†) because the membrane potential was becoming more positive. Therefore, the potentiometric experiments confirmed that the ion-selective membranes were properly operating in all devices, aiding the elucidation of the mechanisms underlying the chemiresistive response.

Table 2 summarizes the sensor performances in both operating modes, chemiresistive and potentiometric modes of the same device for each analyte under the same condition. Both modes yield the same concentration ranges for nitrate, nitrite and ammonium and have very similar response times. The only drawback of the chemiresistive methods is the recovery time of the ammonium sensor. It potentiometrically recovers in 140 seconds while it takes 900 seconds to recover chemire-

Table 2 Chemiresistive response of nitrite, nitrate and ammonium sensors compared with their potentiometric response using the same device for both methods

		Dynamic range (ppm)	Response time (s)	Recovery time (s)
Nitrate sensor	Chemiresistive response	2.2–220	52	47
	Potentiometric response	2.2–220	56	132
Nitrite sensor	Chemiresistive response	0.067–67	66	78
	Potentiometric response	0.067–67	73	80
Ammonium sensor	Chemiresistive response	0.01–100	61	926
	Potentiometric response	0.01–100	45	140

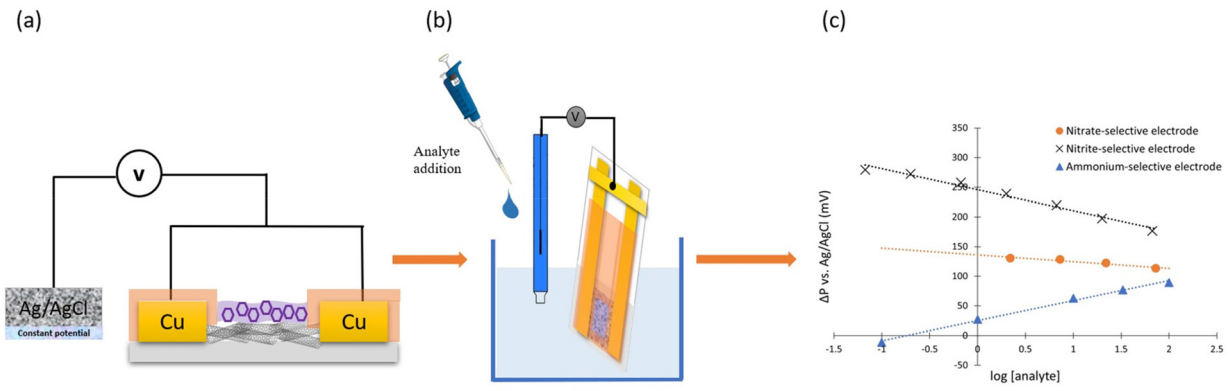

Fig. 6 Fabricated ion-selective electrodes *vs.* a reference electrode for ion detection in water, their responses and their sensing mechanisms based on phase-boundary potential model: (a) a cross-sectional view of the ISE device consisting of a glass support, a carbon nanotube network, two copper contact pads, dielectric material, and ion-selective membrane with the target analyte-related ionophore, (b) a schematic of analyte measurement set-up, (c) responses of nitrate, nitrite and ammonium SC-ISEs.

sistively. It can be concluded that the chemiresistive method for cations and anions measurements in aqueous solutions is feasible without the need for a reference electrode.

3.8. Characterization of bare and blank sensor

The sensitivity of bare and blank chemiresistive devices to nitrogen species was investigated, and their responses were compared to devices covered with ion-selective membranes. Each type of experiment was conducted three times with each of three sets of sensors to ensure accuracy and reproducibility of the results. Each set included 6 devices: one device with a pristine CNT film, a device made with the CNT–TPM composite (both as bare sensors), a CNT–TPM device covered with a layer of blank membrane (contains the same components of ion-selective membranes except the ionophore), one sensor with a film of CNT–TPM composite which covered with the nitrate-selective membrane, one with the nitrite-selective membrane and one with the ammonium-selective membrane. To provide a stable chemical environment, a 200 ppm solution of Tris-acetate buffer at pH 6 was used as a background solution. After running the experiment and achieving a stable current for all sensors, they were exposed to 10 ppm of nitrate, nitrite, ammonium and free chlorine, respectively. In the last step, free chlorine (a strong oxidizing agent) was added as a control to verify that our devices are working correctly and are sealed properly after covering the surface with membrane.[27] As it can be observed in Fig. 7, both bare sensors have a very weak and nonselective response to the addition of 10 ppm of each of the three nitrogen species while a significant response was seen for free chlorine which is confirming that the sensors are operating correctly. This sharp increase is due to the fact that free chlorine is strongly electron-withdrawing, thus charge-transfer doping (oxidizing) the CNT film.[25] As expected, the film covered by a blank membrane did not react with any of the analytes even with free chlorine because it was protected and not in direct contact with the solution (Fig. 7). In contrast, the responses of the fabricated ion-selective chemiresistive devices to 10 ppm of nitrate, nitrite and ammonium are quite substantial. All three sensors showed a drop in current. These results

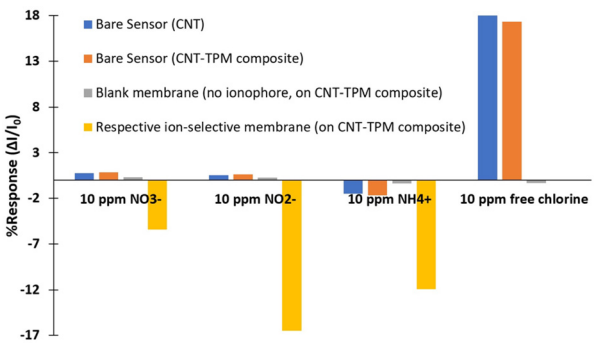

Fig. 7 Response of bare sensor (CNT and CNT–TPM composite) and blank membrane in 200 ppm Tris-acetate buffer at pH 6 upon addition of nitrite, nitrate, ammonium, and free chlorine.

are relevant for the further elucidation of the mechanisms underlying the sensor responses.

3.9. Sensing mechanism of ion-selective chemiresistive devices

The mechanisms by which our chemiresistive devices respond to the different analytes can be understood by considering the properties of the CNT films and membranes as well as the responses of the bare, blank, and ion-selective membrane covered sensing devices upon addition of the respective analytes (Fig. 8). Since the air-brushed CNT network is p-doped by ambient species (molecular oxygen, surface defects), holes are the majority charge carriers. In case of nitrate and nitrite, the respective membranes are positively charged due to having hydrophobic ionophores or additives in their compositions. Studies on IS-FETs have reported that the addition of positively charged membranes on top of p-doped CNT films can result in strong hole repulsion, flipping the net doping state of the film to n-type, so that electrons become the dominant charge carriers at the surface of the percolation network.[78,79] When negatively charged nitrate or nitrite anions are added to the solution, they are captured and transported by the ionophores through the membrane. Thus, a negative potential builds up across the membrane and electrostatic gating of the CNT film occurs, resulting in a decrease in negative charge carrier density on the surface. The chemiresistive current thus drops in response to increased nitrate or nitrite concentrations (Fig. 8c–e). Simultaneously, nitrate and nitrite could also act as oxidizing agents at higher concentrations and accept electrons from the CNT film, further contributing to the decrease in current.[80] This effect is less probable since adsorption of anions onto a negatively charged surface is unfavourable. The fast recovery of the nitrate and nitrite sensors supports the notion that no adsorption is occurring at the interface. However, this adsorption and charge transfer mechanism manifests itself in the responses of bare and blank devices during nitrate and nitrite measurements at higher concentrations (Fig. 3a, 4a and 7). Bare or blank sensors which are not covered with positively charged membranes have p-doped surfaces and adsorption of some nitrate and nitrite ions can occur at higher concentrations, withdrawing some electrons from the surface and p-doping it. Therefore, a slight increase can be observed in bare and blank sensor responses. Fig. 7 clearly shows that the amount of the increase in bare response to nitrate is higher than nitrite due to its higher oxidizing power. In summary, the sensor response is the combination of electrostatic gating and electron withdrawing interactions. Since nitrate and nitrite are weak oxidizers and CNT surface is negatively charged, the contribution of electron withdrawing mechanism to the sensor response is negligibly small. Electrostatic gating is the dominant mechanism in nitrate and nitrite sensors.

In the sensors covered with ammonium-selective membranes, the ionophores act as ammonium ion carriers, bring them into the membrane and close to the CNT film due to the tendency of positively charged ions to interact with oxygen

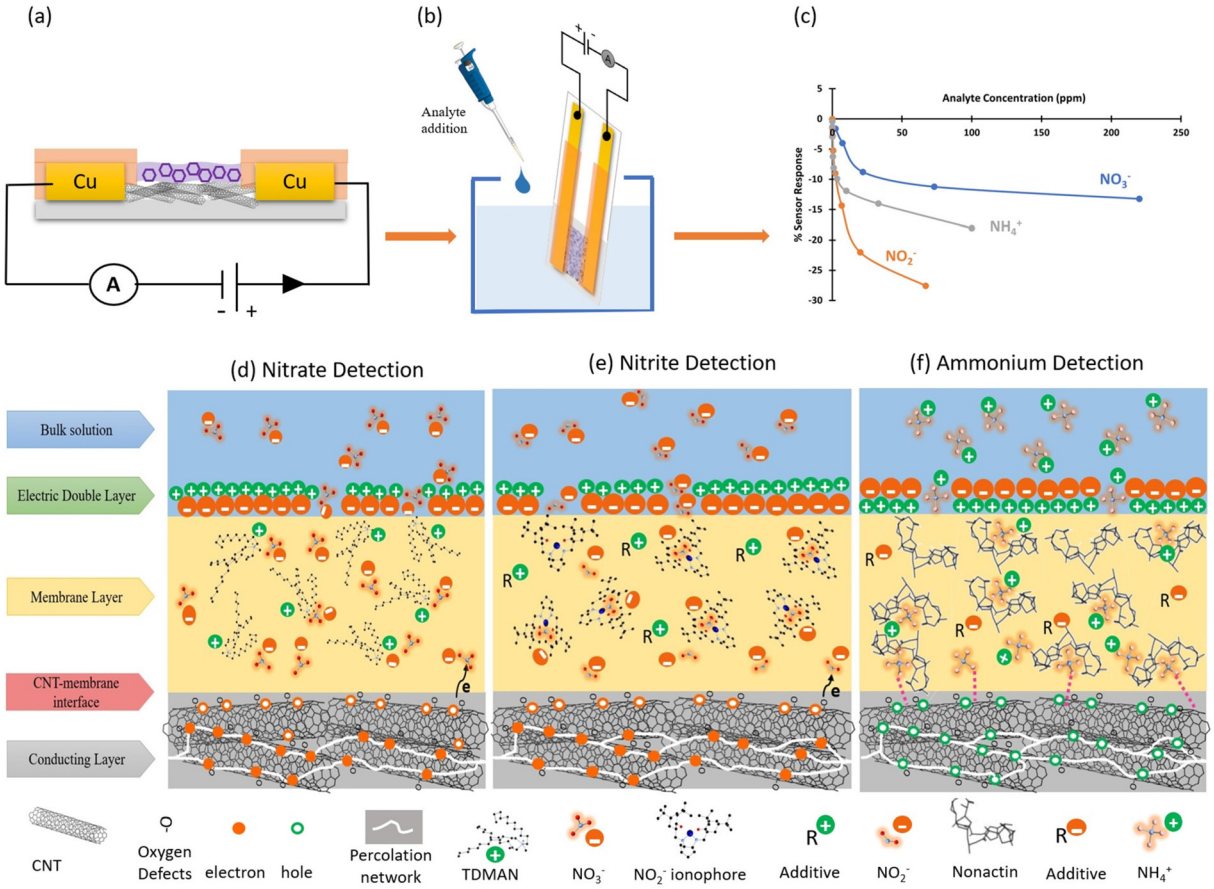

Fig. 8 Designated ion-selective chemiresistive sensor platform for ion detection in water, their responses, and their proposed sensing mechanisms: (a) a cross-sectional view of the chemiresistive device consisting of a glass support, a carbon nanotube network, two copper contact pads, dielectric material, and ion-selective membrane with the target analyte-related ionophore, (b) a schematic of analyte measurement set-up, (c) responses of nitrate, nitrite, and ammonium sensors. (d) Investigation of ion detection mechanism for the proposed chemiresistive platform in aqueous solutions: (d) nitrate detection, (e) nitrite detection, (f) ammonium detection.

defects at the surface. Thus, the build-up of positively charged ammonium ions in the membrane shifts the potential of the membrane towards more positive, electrostatically repulsing holes in the p-doped CNT film and resulting in a decrease in conductance. Another mechanism that can also contribute to the sensor response is adsorption and charge transfer between ammonium and defective CNTs. Experimental and theoretical studies have found that as the density of oxygen defects on the surface increase, ammonium ions are increasingly adsorbed onto the nanocarbon film.[81–84] Bonding can occur between those carbon atoms close to the defects and the hydrogen atoms of the ammonium ions. Computational results suggest that if oxygen atoms interact with hydrogen atoms directly, the adsorption energy between CNT and NH_4^+ decreases, resulting in a less stable film, while the stability of the film is enhanced by the formation of C–H bonds.[83,84] This results in a more p-doped film, since the carbon atoms will share some of their electrons with hydrogen atoms from the adsorbate. Hence, this adsorption and the charge transfer effect add to the density of holes at the surface, thus counteracting the effect of electrostatic gating. As a result of these two opposing mechanisms, a diminished but decreasing trend is observed in the sensor response due to the predominance of the electrostatic gating effect (Fig. 8c and f). The slow recovery of the sensor is due to the adsorption phenomenon. Bare devices also show a decrease at high concentrations due to electrostatic gating. The amount of the decrease is less in the sensors where the surface is covered by a blank membrane (Fig. 5a and 7), but a distinct decrease is nevertheless being observed as the sensor response. Overall, it can be said that the predominant mechanism in all three sensors is electrostatic gating.

Another piece of evidence for the presence of a different mechanism in ammonium detection is the recovery time. The fast response of the nitrate and nitrite sensors is consistent with the proposed sensing mechanism for these sensors based on electrostatic gating. The direct chemical interaction during adsorption and charge transfer with the surface happening in the ammonium sensors requires more time to establish a chemical equilibrium. Thus, when charge transfer is occurring, the recovery is a slow process of desorbing ions from the surface while the chemiresistive current change due to electrostatic gating is much faster.[85]

Table 3 A summary of developed solid-state ISEs with used ionophores in this paper for nitrate, nitrite and ammonium detection in water

	Solid contact	Ionophore	LOD (mol L^{-1})	Detection range (mol L^{-1})	Ref.
Nitrate-selective electrodes	Graphene	TDMAN	3.0×10^{-5}	5.0×10^{-5}–10^{-1}	56
	MWCNTs	TDMAN	2.5×10^{-6}	2.5×10^{-6}–10^{-1}	37
Nitrate-selective chemiresistive sensor	SWCNTs	TDMAN	4.8×10^{-6}	3.6×10^{-5}–3.6×10^{-3}	This study
Nitrite-selective electrodes	Glassy carbon electrode	Cobalt(II) *tert*-butyl-salophen	2×10^{-6}	10^{-5}–10^{-3}	65
	MWCNTs	Cobalt(II) *tert*-butyl-salophen	10^{-6}	10^{-6}–10^{-1}	37
Nitrite-selective chemiresistive sensor	SWCNTs	Cobalt(II) *tert*-butyl-salophen	1.4×10^{-6}	1.5×10^{-6}–1.5×10^{-3}	This study
Ammonium-selective electrodes	Pencil	Nonactin	6.0×10^{-6}	10^{-5}–10^{-1}	86
	CNTs	Nonactin	2.6×10^{-7}	10^{-6}–10^{-3}	9
Ammonium-selective chemiresistive sensor	SWCNTs	Nonactin	3.0×10^{-8}	5.6×10^{-7}–5.6×10^{-3}	This study

A summary of recently developed solid contact-ISEs (SC-ISEs) utilizing the same ionophores as used in this study for determination of nitrogen species in water can be found in Table 3. It is interesting to note that the LODs of nitrate and nitrite chemiresistive sensors (4.8×10^{-6} M and 1.4×10^{-6} M, respectively) are quite close to those of available SC-ISEs while ammonium-selective chemiresistive devices exhibited a much lower LOD (3.0×10^{-8} M) even compared to SC-ISE with advanced design (2.6×10^{-7} M), an advantage achieved as a result of the additional charge transfer sensing mechanism. Overall, ion-selective chemiresistive sensors are competitive in their performance with state-of-the-art potentiometric SC-ISEs for ion detection in water while simplifying device design and eliminating the need for reference electrodes.

4. Conclusion

We demonstrated a selective and robust platform for the detection of anions and cations in water using chemiresistors covered with ion-selective membranes. The membranes increased the selectivity and protected the surfaces of the devices in aqueous environments. Moreover, these devices were easy to fabricate and did not require a reference electrode, enhancing their utility and potential for commercialization. Three different types of ion-selective chemiresistive devices for measurement of nitrate, nitrite and ammonium in aqueous solutions were fabricated. The nitrate-selective chemiresistors worked in a range of 2.2–220 ppm of nitrate solution with an LOD of 300 ppb, but they were susceptible to changes in ionic strength. The nitrite-selective chemiresistors had a dynamic response range from 67 ppb to 67 ppm of nitrite ions with an LOD of 64 ppb. Their response time was shorter in higher concentrations. Since hydroxyl is an interferant for the selected nitrite ionophore, the measurement should be performed at pHs lower than 6. The ammonium sensors were more sensitive than nitrate and nitrite with a LOD of 0.5 ppb and an operating range between 10 ppb to 100 ppm of ammonium solutions. Compared to the nitrate and nitrite sensors, the ammonium sensors showed a faster response in lower concentrations due to a difference in response mechanism. For the same reason, the recovery time of the ammonium sensor was longer. The performance of the chemiresistive devices was comparable to potentiometric measurements in terms of measurable range of analyte concentration, interferants, response time and recovery but did not require a reference electrode.

Overall, the developed sensors are cost-effective, easy to fabricate and easy to use with low electricity consumption, suitable for online measurement and well-tested in real samples. Importantly, we introduced a compatible and sensitive substrate to create a proper interface with ion-selective membranes. This platform benefits from an electrical solid-state ion detection method without a reference electrode. The proposed sensors are competitive to other devices (or better), but still in a proof-of-concept stage. Our results can be combined with other progress done in electronics and membranes field to modify the durability and reproducibility of ion-selective sensors.[87–91] In time, we aim to expand the application of chemiresistive devices to the detection of a wide range of ions in aqueous samples.

Author contributions

All authors participated in manuscript review and editing. Peter Kruse administrated the project and provided funding acquisition in addition to contributing to conceptualization and methodology. Maryam Darestani-Farahani contributed to conceptualization, did investigation and formal analysis as well as writing the original draft. P. Ravi Selvaganapathy contributed to methodology, Vinay Patel and Fanqing Ma contributed to investigation.

Conflicts of interest

There are no conflicts to declare.

Acknowledgements

We thank McMaster Manufacturing Research Institute (MMRI) for the use of the Alicona microscope. Scanning electron microscopy was performed at the Canadian Centre for Electron Microscopy, a Canada Foundation for Innovation Major Science Initiatives funded facility (also supported by

NSERC and other government agencies). Ranjith Divigalpitiya at 3M Canada kindly provided the GLC sheets. Funding for this project was provided by NSERC through the Discovery Grant Program and a Collaborative Research and Development Grant, by 3M Canada, by the Ontario Centers of Excellence, as well as by a Canada First Research Excellence Fund project "Global Water Future".

References

1 M. Cuartero and G. A. Crespo, *Curr. Opin. Electrochem.*, 2018, **10**, 98–106.
2 A. Calvo-López, E. Arasa-Puig, M. Puyol, J. M. Casalta and J. Alonso-Chamarro, *Anal. Chim. Acta*, 2013, **804**, 190–196.
3 M. Cuartero, G. A. Crespo and E. Bakker, *Anal. Chem.*, 2015, **87**, 8084–8089.
4 P. Kruse, *J. Phys. D: Appl. Phys.*, 2018, **51**, 203002.
5 M. Cuartero, G. Crespo, T. Cherubini, N. Pankratova, F. Confalonieri, F. Massa, M.-L. Tercier-Waeber, M. Abdou, J. Schäfer and E. Bakker, *Anal. Chem.*, 2018, **90**, 4702–4710.
6 S. A. Jaywant and K. Mahmood Arif, *Sensors*, 2019, **19**, 4781.
7 L. Nuñez, X. Cetó, M. I. Pividori, M. V. B. Zanoni and M. del Valle, *Microchem. J.*, 2013, **110**, 273–279.
8 M. A. P. Mahmud, F. Ejeian, S. Azadi, M. Myers, B. Pejcic, R. Abbassi, A. Razmjou and M. Asadnia, *Chemosphere*, 2020, **259**, 127492.
9 R. Athavale, I. Kokorite, C. Dinkel, E. Bakker, B. Wehrli, G. A. Crespo and A. Brand, *Anal. Chem.*, 2015, **87**, 11990–11997.
10 WHO, *Guidelines for drinking-water quality*, 2022, vol. 33.
11 R. Paolesse, S. Nardis, D. Monti, M. Stefanelli and C. Di Natale, *Chem. Rev.*, 2017, **117**, 2517–2583.
12 D. W. Kimmel, G. Leblanc, M. E. Meschievitz and D. E. Cliffel, *Anal. Chem.*, 2012, **84**, 685–707.
13 J. Dalmieda, A. Zubiarrain-Laserna, D. Ganepola, P. R. Selvaganapathy and P. Kruse, *Sens. Actuators, B*, 2021, **328**, 129023.
14 I. Fakih, O. Durnan, F. Mahvash, I. Napal, A. Centeno, A. Zurutuza, V. Yargeau and T. Szkopek, *Nat. Commun.*, 2020, **11**, 1–12.
15 W. Wroblewski, M. Dawgul, W. Torbicz and Z. Brzozka, *Proc. SPIE Optoelectron. Electron. Sens. II*, 1997, **3054**, 197–203.
16 W. Chaisrirattanakua, W. Bunjongpru, A. Pankiew, A. Srisuwan, W. Jeamsaksiri, E. Chaowicharat, N. Thornyanadacha, P. Pengpad, M. Horprathum and D. Phromyothin, *Appl. Surf. Sci.*, 2020, **512**, 145664.
17 X. Chen, H. Pu, Z. Fu, X. Sui, J. Chang, J. Chen and S. Mao, *Environ. Sci. Nano*, 2018, **5**, 1990–1999.
18 S. Chen, Y. Tang, K. Zhan, D. Sun and X. Hou, *Nano Today*, 2018, **20**, 84–100.
19 A. Mohtasebi and P. Kruse, *Phys. Sci. Rev.*, 2018, **3**, 1–13.
20 T. Pham, Y. Chen, J. Lopez, M. Yang, T. T. Tran and A. Mulchandani, *Biosensors*, 2021, **11**, 1–13.
21 N. Jaffrezic-Renault and S. V. Dzyadevych, *Sensors*, 2008, **8**, 2569–2588.
22 V. Mani, A. P. Periasamy and S. M. Chen, *Electrochem. Commun.*, 2012, **17**, 75–78.
23 S. J. Choi and I. D. Kim, *Electron. Mater. Lett.*, 2018, **14**, 221–260.
24 J. Dalmieda, A. Zubiarrain-Laserna, D. Saha, P. R. Selvaganapathy and P. Kruse, *J. Phys. Chem. C*, 2021, **125**, 21112–21123.
25 A. Mohtasebi, A. D. Broomfield, T. Chowdhury, P. R. Selvaganapathy and P. Kruse, *ACS Appl. Mater. Interfaces*, 2017, **9**, 20748–20761.
26 A. Zubiarrain-Laserna, S. Angizi, M. A. Akbar, R. Divigalpitiya, P. R. Selvaganapathy and P. Kruse, *RSC Adv.*, 2022, **12**, 2485–2496.
27 L. H. H. Hsu, E. Hoque, P. Kruse and P. R. Selvaganapathy, *Appl. Phys. Lett.*, 2015, **106**, 063102.
28 V. Patel and P. R. Selvaganapathy, *Sens. Actuators, B*, 2021, **349**, 130789.
29 S. Angizi, E. Y. C. Yu, J. Dalmieda, D. Saha, P. R. Selvaganapathy and P. Kruse, *Langmuir*, 2021, **37**, 12163–12178.
30 G. A. Crespo, *Electrochim. Acta*, 2017, **245**, 1023–1034.
31 D. T. Jackson and P. N. Nelson, *J. Mol. Struct.*, 2019, **1182**, 241–259.
32 J. Bobacka, A. Ivaska and A. Lewenstam, *Chem. Rev.*, 2008, **108**, 329–351.
33 A. A. Shul'ga, B. Ahlers and K. Cammann, *J. Electroanal. Chem.*, 1995, **395**, 305–308.
34 U. Trebbe, M. Niggemann, K. Cammann, G. C. Fiaccabrino, M. Koudelka-Hep, S. Dzyadevich and O. Shulga, *Anal. Bioanal. Chem.*, 2001, **371**, 734–739.
35 Government of Ontario, Provincial Water Quality Monitoring Network Website.
36 E. Hoque, T. Chowdhury and P. Kruse, *Surf. Sci.*, 2018, **676**, 61–70.
37 D. Yuan, A. H. C. Anthis, M. Ghahraman Afshar, N. Pankratova, M. Cuartero, G. A. Crespo and E. Bakker, *Anal. Chem.*, 2015, **87**, 8640–8645.
38 A. Bratov, N. Abramova and C. Domínguez, *Anal. Chim. Acta*, 2004, **514**, 99–106.
39 R. Tang, Y. Shi, Z. Hou and L. Wei, *Sensors*, 2017, **17**, 882.
40 M. Novell, M. Parrilla, A. Crespo, F. X. Rius and F. J. Andrade, *Anal. Chem.*, 2012, **84**, 4695–4702.
41 G. A. Crespo, S. Macho and F. X. Rius, *Anal. Chem.*, 2008, **80**, 1316–1322.
42 F. X. Rius-Ruiz, G. A. Crespo, D. Bejarano-Nosas, P. Blondeau, J. Riu and F. X. Rius, *Anal. Chem.*, 2011, **83**, 8810–8815.
43 S. S. M. Hassan, A. G. Eldin, A. E. G. E. Amr, M. A. Al-Omar, A. H. Kamel and N. M. Khalifa, *Sensors*, 2019, **19**, 3891.
44 K. Melzer, A. M. Münzer, E. Jaworska, K. Maksymiuk, A. Michalska and G. Scarpa, *Analyst*, 2014, **139**, 4947–4954.
45 K. R. Moonoosawmy and P. Kruse, *J. Am. Chem. Soc.*, 2008, **130**, 13417–13424.

46 A. Tchernatinsky, S. Desai, G. U. Sumanasekera, C. S. Jayanthi, S. Y. Wu, B. Nagabhirava and B. Alphenaar, *J. Appl. Phys.*, 2006, **99**, 034306.
47 P. G. Collins, K. Bradley, M. Ishigami and A. Zettl, *Science*, 2000, **287**, 1801–1804.
48 L. Brownlie and J. Shapter, *Carbon*, 2018, **126**, 257–270.
49 E. J. R. Sudhölter, R. Huis, G. R. Hays and N. C. M. Alma, *J. Colloid Interface Sci.*, 1985, **103**, 554–560.
50 H. C. Kim, S. K. Kim, J. T. Kim, K. Y. Rhee and J. Kathi, *J. Macromol. Sci., Part B: Phys.*, 2010, **49**, 132–142.
51 H. Yuvaraj, Y. T. Jeong, H. G. Kim, Y. S. Gal, S. S. Hong and K. T. Lim, *Mol. Cryst. Liq. Cryst.*, 2010, **532**, 72–82.
52 H. Ebrahimi, H. Roghani-Mamaqani and M. Salami-Kalajahi, *J. Therm. Anal. Calorim.*, 2018, **132**, 513–524.
53 J. Zou, J. Liu, A. S. Karakoti, A. Kumar, D. Joung, Q. Li, S. I. Khondaker, S. Seal and L. Zhai, *ACS Nano*, 2010, **4**, 7293–7302.
54 S. Najafi-Shoa, H. Roghani-Mamaqani, M. Salami-Kalajahi, R. Azimi and M. Gholipour-Mahmoudalilou, *J. Mater. Sci.*, 2016, **51**, 9057–9073.
55 P. Zou, G.-Y. Shi and C.-Y. Pan, *J. Polym. Sci., Part A: Polym. Chem.*, 2009, **47**, 3669–3679.
56 W. Tang, J. Ping, K. Fan, Y. Wang, X. Luo, Y. Ying, J. Wu and Q. Zhou, *Electrochim. Acta*, 2012, **81**, 186–190.
57 USEPA-9210A, U.S. Environ. Prot. Agency, 2007, 1–12.
58 World Health Organization, *Drinking Water*, 2003, **2**, 21.
59 S. Singh, A. G. Anil, V. Kumar, D. Kapoor, S. Subramanian, J. Singh and P. C. Ramamurthy, *Chemosphere*, 2022, **287**, 131996.
60 D. A. Armbruster and T. Pry, *Clin. Biochem. Rev.*, 2008, **29**, S49–S52.
61 G. L. Long and J. D. Winefordner, *Anal. Chem.*, 1983, **55**, 712A–724A.
62 A. D'Amico, C. Di Natale and P. M. Sarro, *Sens. Actuators, B*, 2015, **207**, 1060–1068.
63 A. Ivanova and K. Mikhelson, *Sensors*, 2018, **18**, 2062.
64 N. Pankratova, M. Ghahraman Afshar, D. Yuan, G. A. Crespo and E. Bakker, *ACS Sens.*, 2016, **1**, 48–54.
65 B. Néel, M. Ghahraman Asfhar, G. A. Crespo, M. Pawlak, D. Dorokhin and E. Bakker, *Electroanalysis*, 2014, **26**, 473–480.
66 M. Pietrzak and M. E. Meyerhoff, *Anal. Chem.*, 2009, **81**, 3637–3644.
67 USEPA-9216, U.S. Environ. Prot. Agency, 2007, 245.
68 N. Pankratova, M. Cuartero, T. Cherubini, G. A. Crespo and E. Bakker, *Anal. Chem.*, 2017, **89**, 571–575.
69 M. S. Ghauri and J. D. R. Thomas, *Analyst*, 1994, **119**, 2323–2326.
70 A. Calvo-López, O. Ymbern, M. Puyol, J. M. Casalta and J. Alonso-Chamarro, *Anal. Chim. Acta*, 2015, **874**, 26–32.
71 T. Guinovart, A. J. Bandodkar, J. R. Windmiller, F. J. Andrade and J. Wang, *Analyst*, 2013, **138**, 7031–7038.
72 World Health Organization, *Drinking Water*, 2003, **2**, 1–16.
73 J. Febrianto, A. N. Kosasih, J. Sunarso, Y. H. Ju, N. Indraswati and S. Ismadji, *J. Hazard. Mater.*, 2009, **162**, 616–645.
74 M. Cuartero, N. Colozza, B. M. Fernández-Pérez and G. A. Crespo, *Analyst*, 2020, **145**, 3188–3210.
75 R. Bauld, D. Y. W. Choi, P. Bazylewski, R. Divigalpitiya and G. Fanchini, *J. Mater. Chem. C*, 2018, **6**, 2901–2914.
76 S. Ezugwu, M. S. Ahmed, R. Bauld, R. Divigalpitiya and G. Fanchini, *Thin Solid Films*, 2013, **534**, 520–528.
77 M. S. Ahmed, S. Ezugwu, R. Divigalpitiya and G. Fanchini, *Carbon*, 2013, **61**, 595–601.
78 J. Kim, Q. Liu and T. Cui, *J. Microelectromech. Syst.*, 2020, **29**, 966–971.
79 J. Kim, Q. Liu and T. Cui, *Org. Electron.*, 2020, **78**, 105551.
80 T. Ketolainen, V. Havu, E. Jónsson and M. J. Puska, *Phys. Rev. Appl.*, 2018, **9**, 34010.
81 C. W. Jang, Y. T. Byun and Y. M. Jhon, *J. Nanosci. Nanotechnol.*, 2012, **12**, 1765–1769.
82 O. Moradi and K. Zare, *Fullerenes, Nanotubes Carbon Nanostruct.*, 2013, **21**, 449–459.
83 Q. Yin, L. Si, R. Wang, Z. Zhao, H. Li and Z. Wen, *Chemosphere*, 2022, **287**, 132294.
84 Q. Yin, L. Si, R. Wang, Z. Zhao and H. Li, *Fuel*, 2022, **325**, 124873.
85 J. Chang, H. Pu, S. A. Wells, K. Shi, X. Guo, G. Zhou, X. Sui, R. Ren, S. Mao, Y. Chen, M. C. Hersam and J. Chen, *Mol. Syst. Des. Eng.*, 2019, **4**, 491–502.
86 T. Fayose, L. Mendecki, S. Ullah and A. Radu, *Anal. Methods*, 2017, **9**, 1213–1220.
87 Y. Huang, X. Wang, W. Xiang, T. Wang, C. Otis, L. Sarge, Y. Lei and B. Li, *Environ. Sci. Technol.*, 2022, **56**, 5334–5354.
88 B. Li, Y. Fan, Y. Huang, W. Linthicum, F. Liu, A. O'Reilly Beringhs, Y. Dang, Z. Xu, S. Y. Chang, J. Ling, B. D. Huey, S. L. Suib, A. W. K. Ma, P. X. Gao, X. Lu, Y. Lei and M. T. Shaw, *ACS Sens.*, 2020, **5**, 3182–3193.
89 T. Wang, C. Cui, Y. Huang, Y. Fan, Z. Xu, L. Sarge, C. Bagtzoglou, C. Brückner, P. Gao and B. Li, *Environ. Sci. Nano*, 2022, **9**, 2149–2160.
90 Y. Fan, X. Qian, X. Wang, T. Funk, B. Herman, J. R. McCutcheon and B. Li, *J. Membr. Sci.*, 2022, **643**, 119997.
91 X. Wang, Y. Fan, Y. Huang, J. Ling, A. Klimowicz, G. Pagano and B. Li, *ACS ES&T Water*, 2021, **1**, 530–541.